Self-Ignition of S.I. Engine Model Fuels: A Shock Tube Investigation at High Pressure

K. FIEWEGER,* R. BLUMENTHAL, and G. ADOMEIT
Institut für Allgemeine Mechanik, RWTH Aachen D-52056 Aachen, Germany

The self-ignition of several spark-ignition (SI) engine fuels (*iso*-octane, methanol, methyl *tert*-butyl ether and three different mixtures of *iso*-octane and *n*-heptane), mixed with air, was investigated experimentally under relevant engine conditions by the shock tube technique. Typical modes of the self-ignition process were registered cinematographically. For temperatures relevant to piston engine combustion, the self-ignition process always starts as an inhomogeneous, deflagrative mild ignition. This instant is defined by the ignition delay time, τ_{defl}. The deflagration process in most cases is followed by a secondary explosion (DDT). This transition defines a second ignition delay time, τ_{DDT}, which is a suitable approximation for the chemical ignition delay time, if the change of the thermodynamic conditions of the unburned test gas due to deflagration is taken into account. For *iso*-octane at $p = 40$ bar, a NTC (negative temperature coefficient), behaviour connected with a two step (cool flame) self-ignition at low temperatures was observed. This process was very pronounced for rich and less pronounced for stoichiometric mixtures. The results of the τ_{DDT} delays of the stoichiometric mixtures were shortened by the primary deflagration process in the temperature range between 800 and 1000 K. Various mixtures of *iso*-octane and *n*-heptane were investigated. The results show a strong influence of the *n*-heptane fraction in the mixture, both on the ignition delay time and on the mode of self-ignition. The self-ignition of methanol and MTBE (methyl *tert*-butyl ether) is characterized by a very pronounced initial deflagration. For temperatures below 900 K (methanol: 800 K), no secondary explosion occurs. Taking into account the pressure increase due to deflagration, the measured delays τ_{DDT} of the secondary explosion are shortened by up to one order of magnitude. © 1997 by The Combustion Institute

INTRODUCTION

Knocking combustion in spark ignition (SI) engines restricts further improvement of engine efficiency through an increase in the compression ratio. The knocking phenomenon is characterized by noise, caused by strong pressure waves and pressure oscillations in the cylinder, and is transmitted through the engine structure. Because the high thermal and mechanical load of parts of the engine induced by these gasdynamic processes may lead to serious damage, knocking combustion is undesirable.

The knock process and its cause have been the subject of theoretical and experimental research for a long time. Investigations using optical measurement techniques, such as high speed photography, have shown auto-ignition to occur in the unburned, compressed end gas preceeding knock [1–6]. As long as this auto-ignition proceeds inhomogeneously and leads to a hot spot ignition inducing a deflagrative process, it causes only a weak pressure increase and is commonly not termed knock [3]. If auto-ignition leads to a rapid energy release in a sufficiently extended region, it is connected with strong pressure waves (shock waves). These can be observed in typical pressure histories obtained from knocking engine cycles. Hence, the knock phenomenon appears to be the result of the interaction of gasdynamic processes and the exothermic combustion chemistry of the fuel–air system. The latter is strongly influenced by the thermodynamic conditions in the end gas, which are changed by the pressure waves generated by the primary flame (ignited by the spark) or by flame kernels arising from hot spot auto-ignition in the end gas. Consequently, the understanding and the numerical modeling of the knocking process requires a detailed knowledge of the chemical kinetics of the fuel–air system and its coupling with gasdynamic processes under relevant engine conditions.

The self-ignition process of homogeneous fuel–air mixtures under thermodynamic conditions close to those in the end gas of a SI

* Corresponding author.

COMBUSTION AND FLAME 109: 599–619 (1997)

Published by Elsevier Science Inc.

0010-2180/97/$17.00
PII S0010-2180(97)00049-7

engine can be investigated with shock tubes. This experimental device has several advantages. The compression by the incident and the reflected shock wave is sufficiently short to reduce any influences of the compression process. In the present study, the measuring time of a maximum of 12 ms represents a time scale comparable to that available for auto-ignition in an engine. The main parameters controlling the chemical processes like temperature and pressure after compression, equivalence ratio and fuel composition, can be varied independently. Also the gasdynamic processes during self-ignition can be studied either by high-speed photography of a shock tube with large windows, or by recording pressure and band emission signals at different positions in the test section.

Ignition delay times obtained in previous studies [7–9] have recently been used to develop and verify detailed [10] and reduced [11] kinetic mechanisms. The experimental investigations presented here extend these investigations to other fuels and complement them by the shadowgraphic visualisation of the gasdynamic features of the self-ignition process. This is highly relevant to an understanding of the processes connected with engine knock.

Various representative gasoline fuels have been investigated in this study, varying temperature and pressure within a wide range, and also, partially, the equivalence ratio. Because of its significance as a primary reference fuel (PRF), *iso*-octane was investigated in some detail. In order to clarify the influence of the octane number (ON) on both the self-ignition process and the ignition delay time, several mixtures (ON 90, ON 80 and ON 60) of the two primary reference fuels, *iso*-octane and *n*-heptane, were studied. Furthermore, methyl *tert*-butyl ether (MTBE), which increasingly replaces benzene in gasoline, and methanol, which is a promising alternative SI engine fuel, have been investigated.

APPARATUS

All the experimental results were obtained with the reflected shock technique, under the condition of a tailored interface. This led to relatively long measuring times of up to 12 ms. The experimental procedure and the shock tube used for the high pressure experiments are described in [8, 9, 12, 13]. This device was designed to support maximum pressures of up to 700 bar arising from the self-ignition of homogeneous hydrocarbon/air mixtures at initial pressures of 40 bar. The test section is equipped at different positions with acceleration-compensated piezoelectric pressure transducers and opposite quartz windows for the registration of CH-radical band emission at 431 nm.

A second shock tube of square cross-section (54 mm) and a test section equipped with large windows, covering the entire cross-section along a length of 200 mm next to the end wall, was used for the shadowgraphic visualisation of the self-ignition process at initial pressures up to 15 bar. The photographs were obtained with a Cranz-Schardin camera, which allows a sequence of 24 pictures at a frequency of up to 10 MHz.

The main measurement position in both tubes is at 15 mm in front of the end wall of the low pressure part. The temperature behind the reflected shock was calculated from the velocity of the incident shock. This was obtained from the signals of three fast thin film heat transfer gauges which are mounted flush to the wall along the tube axis. For the calculation of the temperature, T_5, of the test gas behind the reflected shock, real gas properties of the test gas were taken into account using the data and procedures in [14, 15].

RESULTS AND DISCUSSION

Gasdynamic Features of the Self-Ignition Process in a Shock Tube

Auto-ignition of hydrocarbon/air mixtures in engines and in experimental devices such as shock tubes and rapid compression machines, proceeds in different modes depending on the temperature, pressure, fuel, geometry, impurities and other factors [4, 6, 16, 23]. Hence, the self-ignition behaviour of a fuel in air is characterized not only by the ignition delay time, but also by the gasdynamic features of the auto-ignition process. A fundamental classification of the modes of self-ignition has been given by Oppenheim [16, 17].

In order to interpret the results from our high-pressure shock tube and to find a uniform criterion for the determination of ignition delay times for all experiments with several types of self-ignition, we performed a set of experiments using the shock tube with square cross-section and large windows in the test section. The self-ignition process was visualized by the Cranz–Schardin camera. Due to the lower mechanical strength of this tube, all experiments were at an initial pressure, p_5, after compression of about 13 bar. A comprehensive survey of the results is to be found in [18].

Figures 1–5 consist of a series of shadowgraphs. Each frame shows the whole cross-section of the test chamber (height 54 mm) with the end wall of the shock tube at the right. The corresponding signals of pressure and CH-band emission at 431 nm (negative signals) are plotted for several positions in the test section, which are marked below the photographs. The number of the measuring position can also be

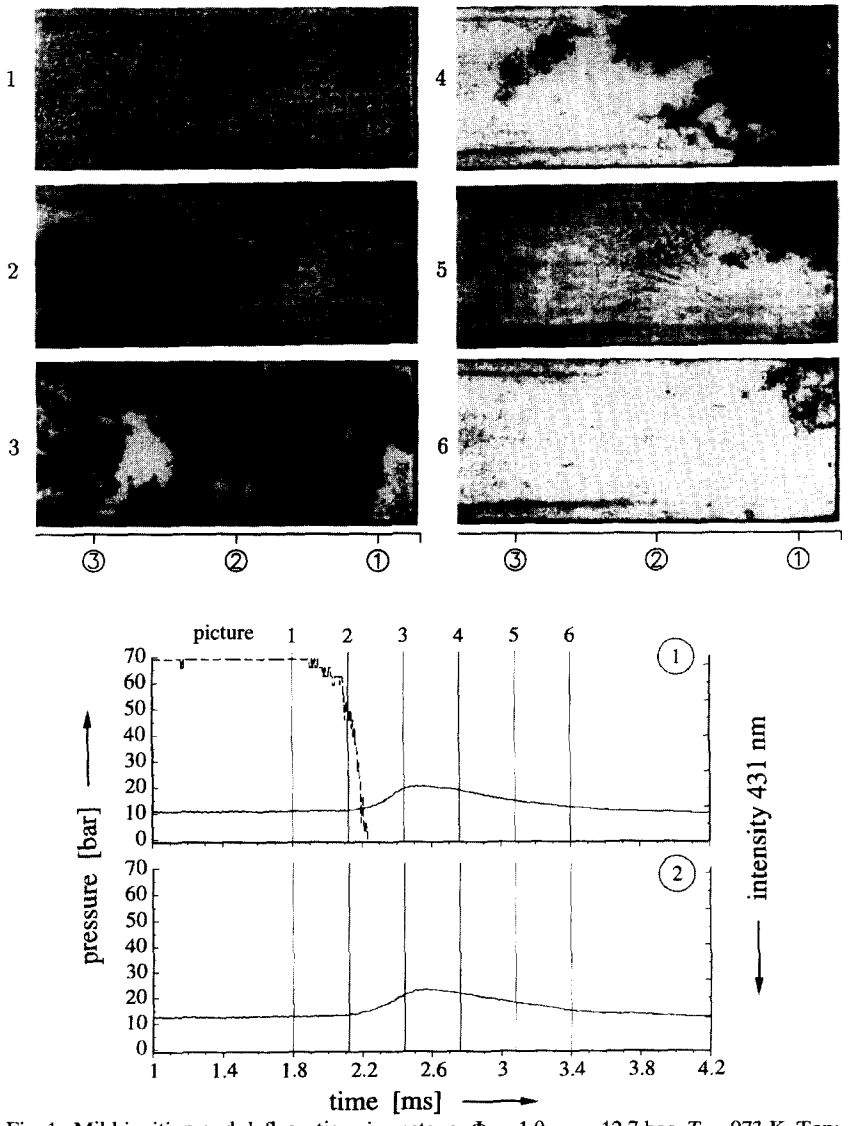

Fig. 1. Mild ignition and deflagration, *iso*-octane, $\Phi = 1.0$, $p = 12.7$ bar, $T = 973$ K. Top: Series of shadowgraphs, time between frames $\Delta t = 320$ μs. Bottom: Pressure and CH-band emission signals at different positions in test section.

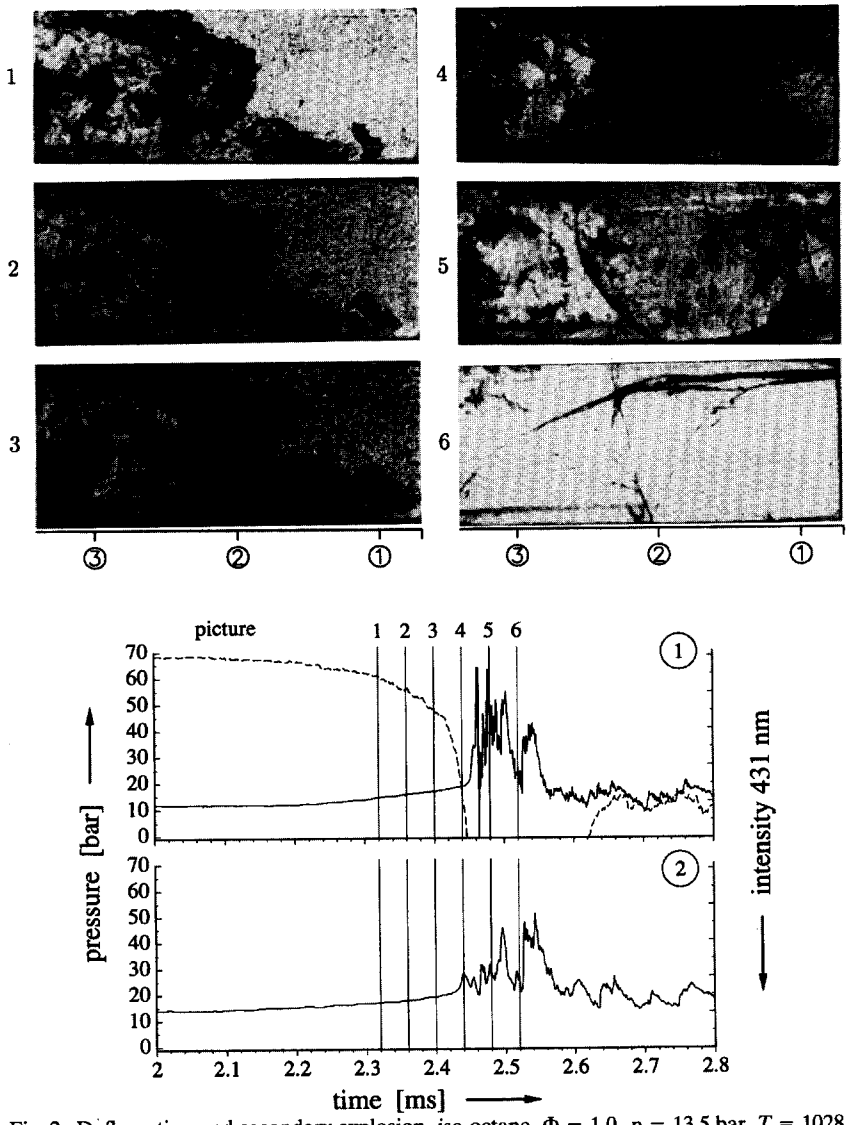

Fig. 2. Deflagration and secondary explosion, *iso*-octane, $\Phi = 1.0$, $p = 13.5$ bar, $T = 1028$ K. Top: Series of shadowgraphs, time between frames $\Delta t = 40$ μs. Bottom: Pressure and CH-band emission signals at different positions in test section.

found in the plots. In addition, the instants of the pictures are marked by vertical lines and the corresponding number.

At lower temperatures—which are representative of the thermodynamic conditions in engines—the self-ignition commences as a so called hot spot mild ignition. Due to the inhomogeneities which might arise in temperature, radical concentration, or particles in the test gas, a deflagrative process develops after local self-ignition at hot spots or exothermic centers which leads to one or several flame kernels. This deflagration induces only a smooth pressure rise. In the shock tube, the main cause of temperature inhomogeneities is the interaction of the reflected shock wave with the boundary layer arising from the incident shock [19, 20]. Also, by this interaction, cold gas at the side wall is transported towards the end wall of the shock tube. This may explain the fact that at lower temperatures, the first self-ignition does not necessarily occur near the end wall of the test section, as would be expected for an ideal shock tube. At lower temperatures and increasing ignition delay times, the number of the flame kernels decreases, which may be

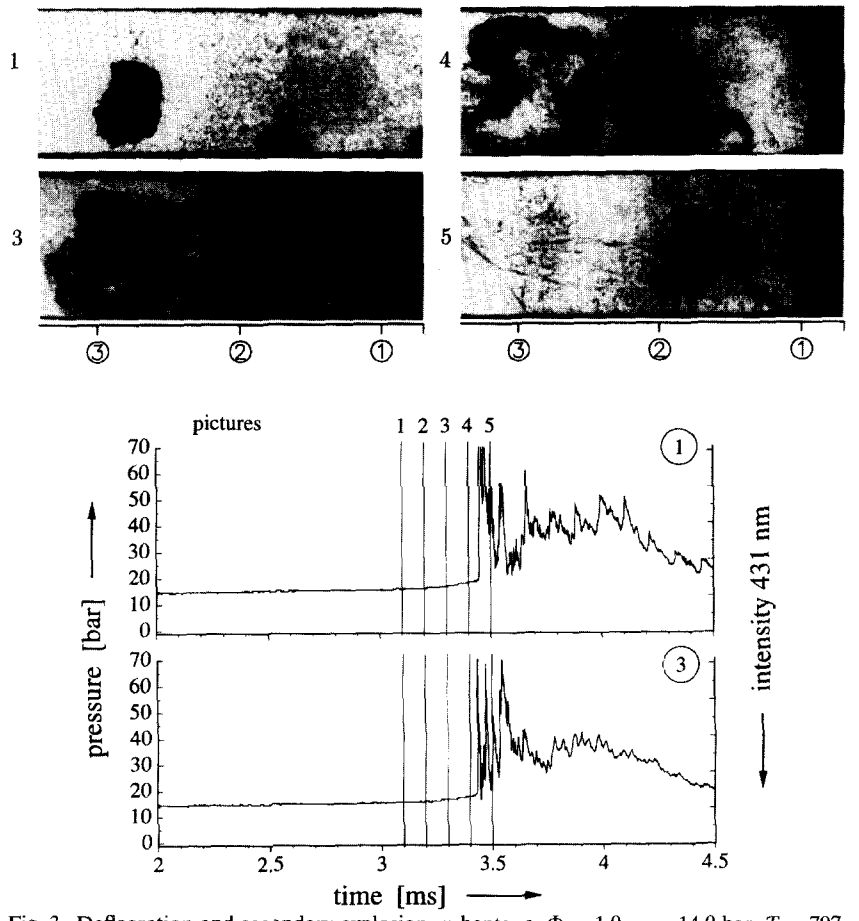

Fig. 3. Deflagration and secondary explosion, *n*-heptane, $\Phi = 1.0$, $p = 14.0$ bar, $T = 797$ K. Top: Series of shadowgraphs, time between frames $\Delta t = 100$ μs. Bottom: Pressure signals at different positions in test section.

caused by compensation processes. Also relevant is the effect of catalytic particles leading to inhomogeneous ignition, which has been discussed in the literature [21, 22].

An example of a mild, deflagrative self-ignition process is shown in Fig. 1. In this experiment (*iso*-octane/air, $\Phi = 1.0$, $p = 12.7$ bar, $T = 973$ K), the entire test gas was consumed by the deflagration. The pressure histories show only a smooth increase, with a maximum of about 20 bar. The appearance and the growth of the first flame kernels corresponds to a continuously increasing signal from the CH-band emission.

In its later phase, the initial mild self-ignition process may lead to a secondary explosion of larger volumes of the unburned test gas and a transition to a detonation-like process (DDT, strong ignition). This is connected with strong pressure peaks and steep pressure gradients resulting from shock waves arising from the secondary explosion (explosion in the explosion). This process is illustrated in Figs. 2 and 3 for *iso*-octane and *n*-heptane. Both the shadowgraphs and the pressure signals show the strong pressure waves ($p_{max} \approx 70$ bar) generated by the secondary explosion. Although this process seems to be very similar for both hydrocarbons, comparison of Figs. 2 and 3 illustrates different behaviours of the two primary reference fuels. While at $p_5 \approx 13$ bar, the self-ignition of *iso*-octane was completely deflagrative for temperatures below 1000 K (see Fig. 1), that of *n*-heptane for all the temperatures investigated, showed a fast transition to a detonation-like self-ignition process following

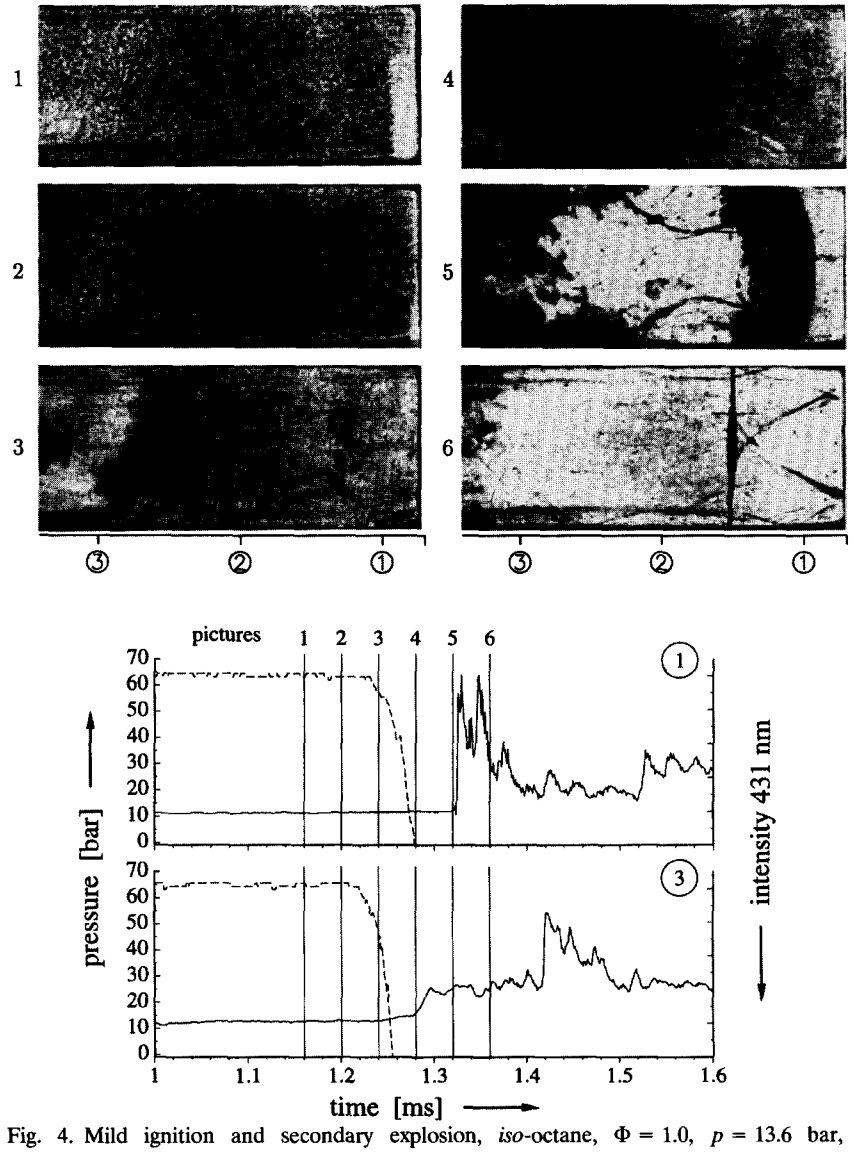

Fig. 4. Mild ignition and secondary explosion, *iso*-octane, $\Phi = 1.0$, $p = 13.6$ bar, $T = 1105$ K. Top: Series of shadowgraphs, time between frames $\Delta t = 10$ μs. Bottom: Pressure and CH-band emission signals at different positions in test section.

a short deflagration. Also, in contradistinction to *iso*-octane, the deflagration of *n*-heptane at 797 K did not lead to an evident pressure increase before the transition. Frame 4 in Fig. 3 shows that a very large volume of the unburned test gas between two flame kernels ignited virtually simultaneously. This different behaviour of the two primary reference fuels is of great relevance for the knocking process in an engine.

At higher temperatures, a very short deflagrative phase was followed by a fast transition to a detonation-like process for both fuels. This is illustrated in Fig. 4 for *iso*-octane at $T = 1100$ K. The secondary explosion occurred in the time interval between frames 4 and 5, almost homogeneously within the whole cross-section of the tube, leading to the formation of a detonation wave that moved rapidly into the unburned test gas. The whole process is also indicated by the pressure and band emission signals.

At very high temperatures, strong ignition [16, 17] occurs, which is a homogeneous explo-

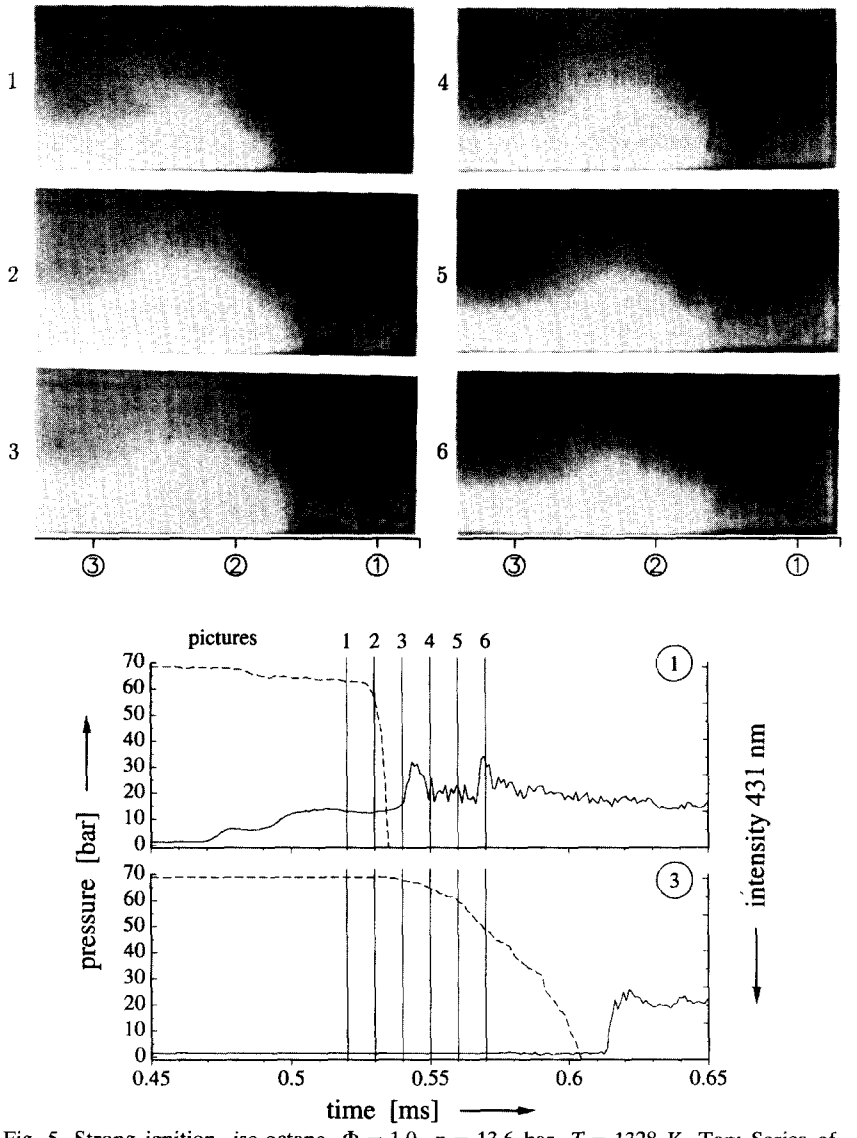

Fig. 5. Strong ignition, *iso*-octane, $\Phi = 1.0$, $p = 13.6$ bar, $T = 1328$ K. Top: Series of shadowgraphs, time between frames $\Delta t = 10$ μs. Bottom: Pressure and CH-band emission signals at different positions in test section.

sion of the reactive mixture, with the instantaneous development of a shock which forms a detonation. Figure 5 shows such a strong ignition for *iso*-octane at $T = 1330$ K. The reflected shock wave moving to the left side can be seen clearly. In frame 2, self-ignition occurred homogeneously in the whole cross-section at the end wall. A detonation was formed, which moved through the unburned gas and caught up with the reflected shock in frame 5. This process is connected with moderate maximum pressures. This type of self-ignition is very similar to an idealized zero-dimensional kinetic modeling, but requires very high temperatures which are of less relevance for engine applications.

Definition of Ignition Delay Times

The different modes of self-ignition observed in the shock tube experiments require appropriate definitions of the ignition delay times. Because the self-ignition process can only be photographically visualised at lower pressures,

at high pressures the different delay times characterizing the self-ignition process must be derived solely from the pressure and emission signals. For all experiments, the start of the ignition delay period was defined by the instant when the reflected shock passed the first pressure transducer 15 mm in front of the end wall.

Figure 6 shows a series of photographs (frames 1, 6, 11: $\Delta t = 200$ μs; 11–14: $\Delta t = 40$ μs) and corresponding pressure and CH-band emission histories at 15 mm in front of the end wall. Again, the vertical lines mark the instants at which pictures were taken during this run. They are numbered at the top of the diagram. The formation of the first flame kernel and its growth can be seen clearly. The first pressure rise starts at frame 6, but the first increase of the emission signal is already recorded at frame 1. As can be seen in this figure and also in Fig. 1, the occurrence of the first flame kernels is always connected with a first increase of the emission signal at 431 nm. Hence, this instant

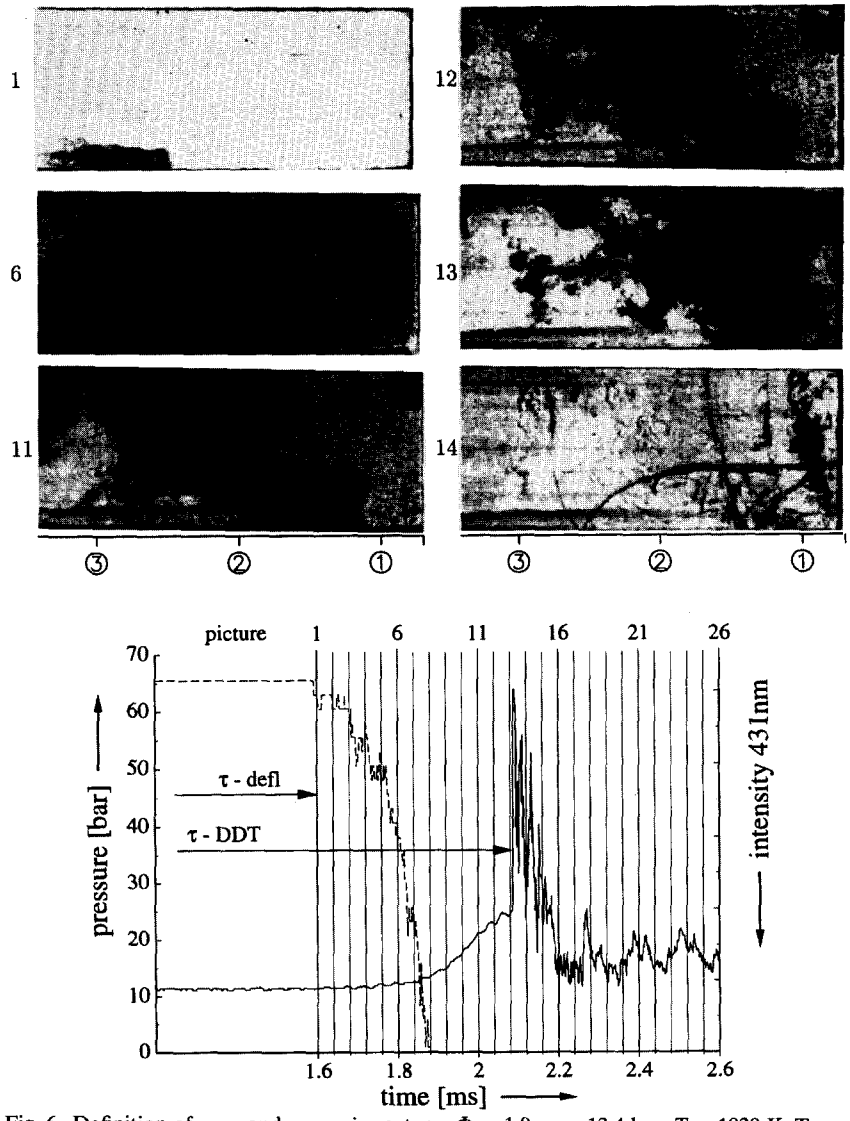

Fig. 6. Definition of τ_{defl} and τ_{DDT}, *iso*-octane, $\Phi = 1.0$, $p = 13.4$ bar, $T = 1029$ K. Top: Series of shadowgraphs, time between frames 1–11: $\Delta t = 200$ μs; 11–14: $\Delta t = 40$ μs. Bottom: Pressure and CH-band emission signals at 15 mm in front of the end wall of the test section.

defines the first ignition delay time, τ_{defl}, which marks the beginning of the inhomogeneous, deflagrative phase. As mentioned above, this process starts from very small localized points of self-ignition. It should be noted that differences in the measured CH-band emission and the real flame kernel development may exist, due to the limited observation area of the emission registration device. Because in the high pressure shock tube, no photographs could be taken and the CH-band emission measured at 15 mm in front of the end wall of the test section was used for the determination of τ_{defl}, the occurrence of flame kernels may be possible earlier than is registered by the CH-band emission measurement. Hence, the delay time τ_{defl} is of minor interest for zero-dimensional kinetic modeling, as the nature of these hot spots and their thermodynamic state is not clear. Nevertheless, this time describes well the self-ignition of hydrocarbon/air mixtures under real conditions, such as those in the end gas of an SI engine, where this hot spot ignition has been observed and described in detail [4].

In Fig. 6, the deflagrative phase proceeds until frame 13, when a secondary explosion arises near the end wall. The ensuing shock waves, reflected at the end wall, can be seen in frame 14 and are indicated in the pressure record. Hence, the instant of the secondary explosion can be determined easily from the pressure records and was used for the determination of a second ignition delay time, τ_{DDT}. As can be seen also in Figs. 2–4, this secondary explosion represents the more or less homogeneous self-ignition of a larger volume of the test gas. Thus, the delay time, τ_{DDT}, can be interpreted as the best approximation for the chemical ignition delay time and was used also in our recent investigations [7, 8].

Especially for SI engine fuels with relatively long ignition delay times, there may be a change of the thermodynamic conditions of the unburned test gas before the secondary explosion occurs, due to the pressure waves resulting from deflagration. This has to be taken into account for the interpretation of the measured τ_{DDT}, as shown in the following example. The pressure history in Fig. 6 shows an increase from 13 up to 25 bar during the deflagrative phase. Assuming isentropic compression, this pressure increase is connected with a simultaneous temperature increase from 1030 K to 1180 K ($\gamma = 1.27$). This change in condition of the still unburned gas will lead to a distinct shortening of the ignition delay time, τ_{DDT}. A quantitative approach to determine the chemical ignition delay time without any influence of deflagration can be made by assuming the dependence $\tau_i = f(T, p)$ in such a way that the relation [24, 25]

$$1 = \int_0^{\tau_{DDT}} \frac{dt}{\tau_i(T(t), p(t))}. \tag{1}$$

holds. This uses the measured pressure histories and assumes isentropic compression for the calculation of the temperature history. Consequently, in the next section, both the ignition delay times and pressure histories will be presented and discussed. Because an evident pressure increase resulting from deflagration was observed only for stoichiometric mixtures in the temperature range between 800 and 1000 K, only in these cases was this evaluation necessary. Diesel fuels, such as *n*-heptane, showed only a short deflagrative phase with no evident pressure increase before the secondary explosion in the whole temperature range of investigation [8].

Two examples of the application of the two definitions of ignition delay, τ_{defl} and τ_{DDT}, are to be found in Figs. 7 and 8. They show typical histories of pressure and CH-band emission recorded 15 mm in front of the end wall of the test section of the high-pressure shock tube. Figure 7 shows the self-ignition process of a stoichiometric MTBE/air mixture at $T = 800$ K and $p = 40$ bar. No secondary explosion occurred in this experiment because either the whole test gas was consumed during the deflagration, or the delay time, τ_{DDT}, was longer than the maximum test time. Figure 8 shows another typical self-ignition process of a stoichiometric *iso*-octane/air mixture at $T = 770$ K and $p = 40$ bar. Although there was a strong CH emission signal after τ_{defl}, there was no pressure increase during the deflagrative phase. Therefore, in this experiment, τ_{DDT} corresponds very well to the chemical ignition delay time as customarily defined.

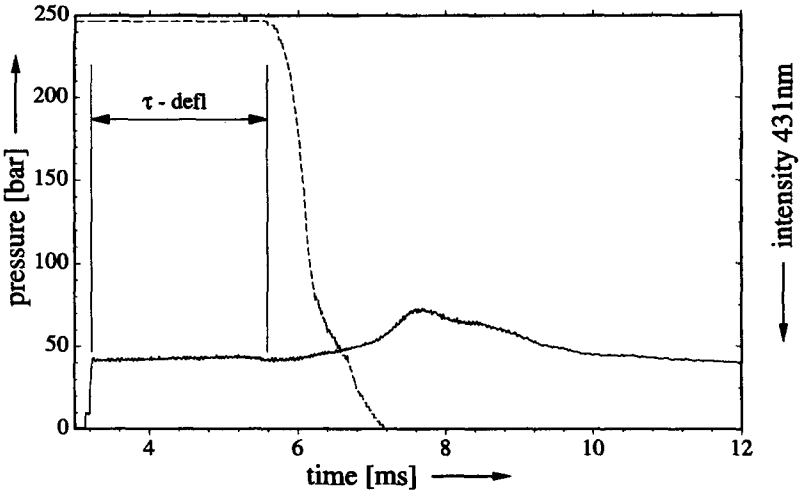

Fig. 7. Mild ignition and deflagration, MTBE, $\Phi = 1.0$, $p = 40$ bar, $T = 800$ K. Pressure and CH-band emission histories.

A third delay time, of great relevance for the chemistry of the hydrocarbon/air mixture investigated, is τ_1, that for the cool flame process (pre-ignition), which occurs during the two-step low-temperature oxidation of some hydrocarbons [23, 27, 31] and is caused by alkylperoxyde radical reactions. The initiation of the cool flame process is recorded by both pressure record, which shows a small but distinctive step-like increase, and the emission signal, which leads to a weak maximum. The delay time, τ_1, can be determined quite precisely from these signals (see Fig. 9).

In contrast to the main ignition described before, the cool flame process is hardly influenced by inhomogeneities. Photographs of this process show that it proceeds relatively homogeneous starting from the end wall of the test section. The front of the cool flame reaction moves with a velocity approximately equal to the velocity of the reflected shock. No flame-like structures could be observed. For all ex-

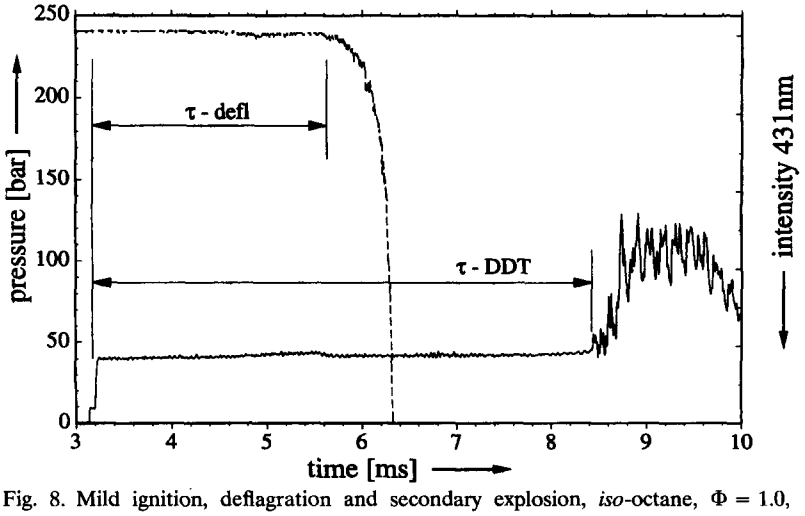

Fig. 8. Mild ignition, deflagration and secondary explosion, *iso*-octane, $\Phi = 1.0$, $p = 40$ bar, $T = 770$ K. Pressure and CH-band emission histories.

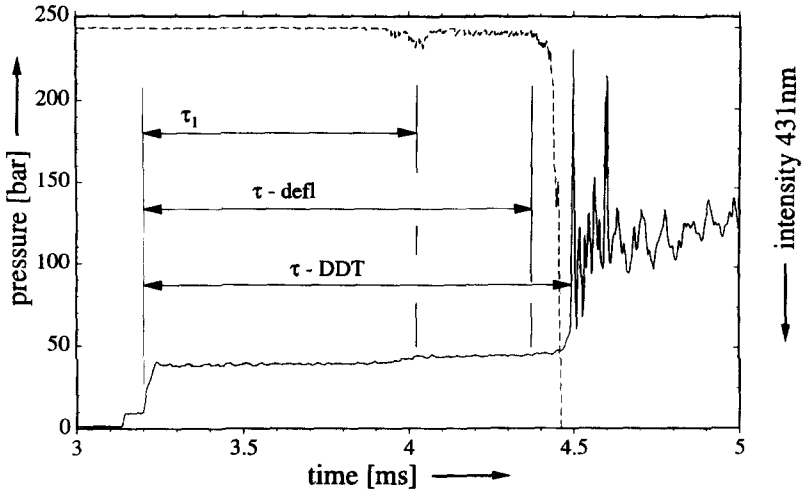

Fig. 9. Cool flame process, mild ignition and secondary explosion, 60% *iso*-octane/40% *n*-heptane, $\Phi = 1.0$, $p = 40$ bar, $T = 780$ K. Pressure and CH-band emission histories.

periments showing a two-step low-temperature self-ignition process, the cool flame appears to be followed by only a short deflagrative phase with negligible pressure increase and an immediately consecutive detonative self-ignition.

Ignition Delay Times

The ignition delay times obtained in the manner described are presented by Arrhenius diagrams in the form of plots of $\log \tau$ versus $1/T_5$.

iso-Octane

Figures 10 and 11 show ignition delay times for stoichiometric *iso*-octane/air mixtures with the pressure varied. The delay times, τ_{DDT}, and τ_1, can be found in Fig. 10, while in Fig. 11, the results for mild ignition, τ_{defl}, are presented. In addition, the pertinent pressure histories are

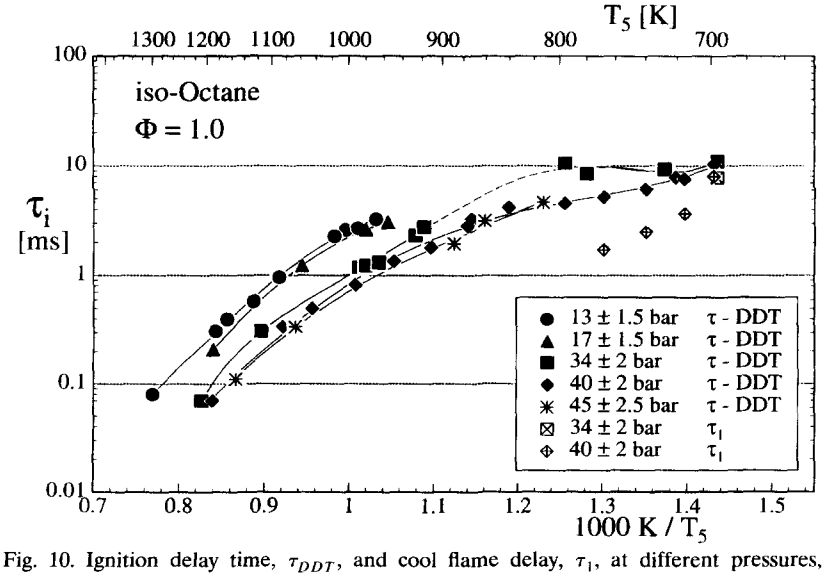

Fig. 10. Ignition delay time, τ_{DDT}, and cool flame delay, τ_1, at different pressures, *iso*-octane, $\Phi = 1.0$.

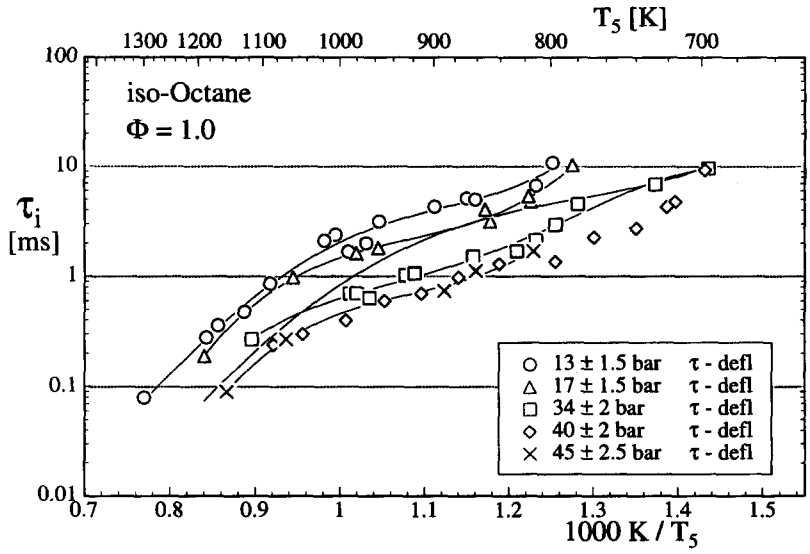

Fig. 11. Ignition delay time, τ_{defl}, at different pressures, *iso*-octane, $\Phi = 1.0$.

plotted for the investigated temperature range and three pressures (13 ± 1.5 bar, 34 ± 2 bar, 40 ± 2 bar) in Figs. 12–14. In these diagrams, a vertical line inside the shaded area under the pressure profiles indicates the beginning of the deflagration, which corresponds to τ_{defl} in Fig. 11. For discussion purposes, the whole temperature range can be divided into three regions.

First, in the high temperature region, $T > \approx 1050$ K, the self-ignition proceeds in a detonative manner similar to that described for Fig. 4. The respective ignition delay times show an approximately linear dependence in the Arrhenius plot. At the higher pressures, the time, τ_{DDT}, becomes shorter, but the slope of the curves is essentially unchanged.

Second, in the intermediate temperature range, ≈ 1050 K $< T < \approx 800$ K, the deflagrative phase of the self-ignition process is very pronounced. This leads to a significant pressure increase, which can be observed for all the pressures in Figs. 12–14. At the lower pressures (13 and 34 bar), there is no secondary explosion for temperatures lower than a limiting value. Due to the pressure and temperature increase during deflagration, the ignition delay times, τ_{DDT}, are shortened considerably in some cases. An estimation of this influence using Eq. 1 shows that at $T = 1000$ K, the value of τ_{DDT} is approximately halved. The pressure increase caused by the deflagrative combustion becomes smaller for decreasing temperatures, so that for $T < 800$ K, τ_{DDT} again becomes identical to the chemical ignition delay time. In Fig. 12, it can be seen that in the temperature range 950–1000 K only small pressure peaks are observed. In these experiments, nearly all the test gas was consumed by the deflagration prior to the secondary explosion. At $p = 34$ bar and $T < 900$ K (Fig. 13), the pressure and temperature increase due to the deflagration is not strong enough to shorten the ignition delay time, τ_{DDT}, to a value smaller than the maximum test time of approximately 12 ms. The test gas either is consumed during the deflagration or the self-ignition process is quenched by the arrival of the expansion wave. The latter arises from the expansion of the driver gas after the breaking of the diaphragm, and is reflected at the end wall of the high pressure part of the shock tube. There is a considerable difference between the two times, τ_{defl} and τ_{DDT}, as can be seen from Figs. 10 and 11. The fact that the first local mild self-ignition leading to deflagration (τ_{defl}) takes place much earlier than the consecutive strong ignition cannot be explained by temperature inhomogeneities alone. Further research is definitely required.

Thirdly, in the low temperature region, T

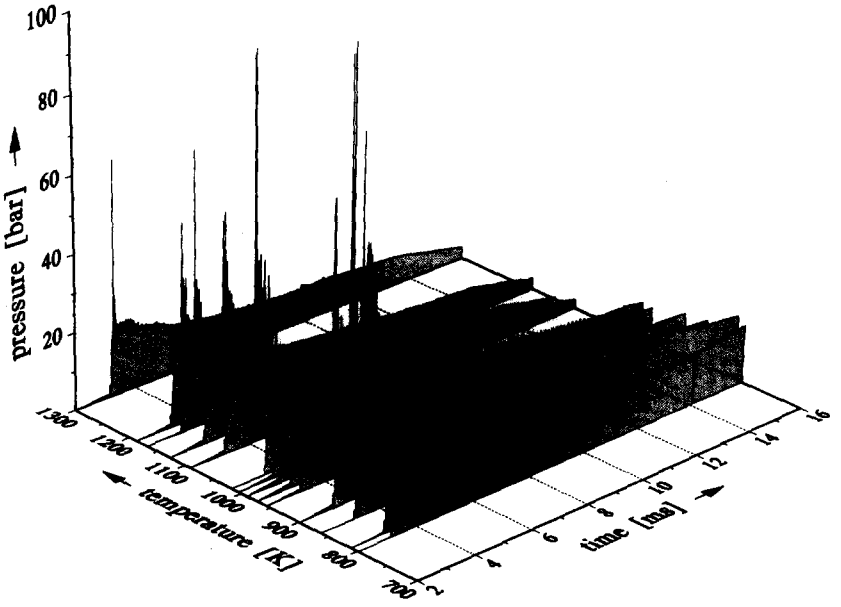

Fig. 12. Pressure histories at different temperatures, *iso*-octane, $\Phi = 1.0$, $p = 13 \pm 1.5$ bar. Vertical lines inside shaded area under pressure profiles mark instant of mild ignition. Signals were obtained at 15 mm in front of end wall.

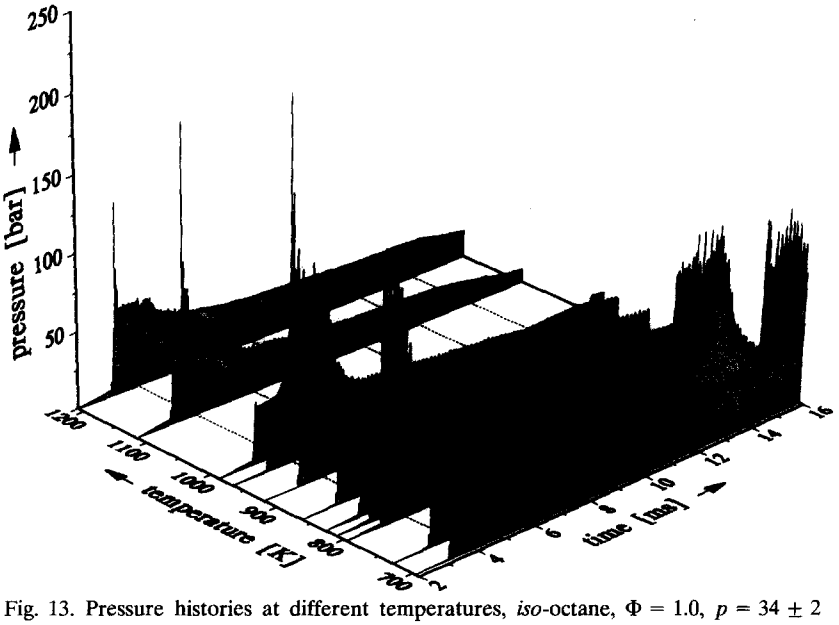

Fig. 13. Pressure histories at different temperatures, *iso*-octane, $\Phi = 1.0$, $p = 34 \pm 2$ bar. Vertical lines inside shaded area under pressure profiles mark instant of mild ignition. Signals were obtained at 15 mm in front of end wall.

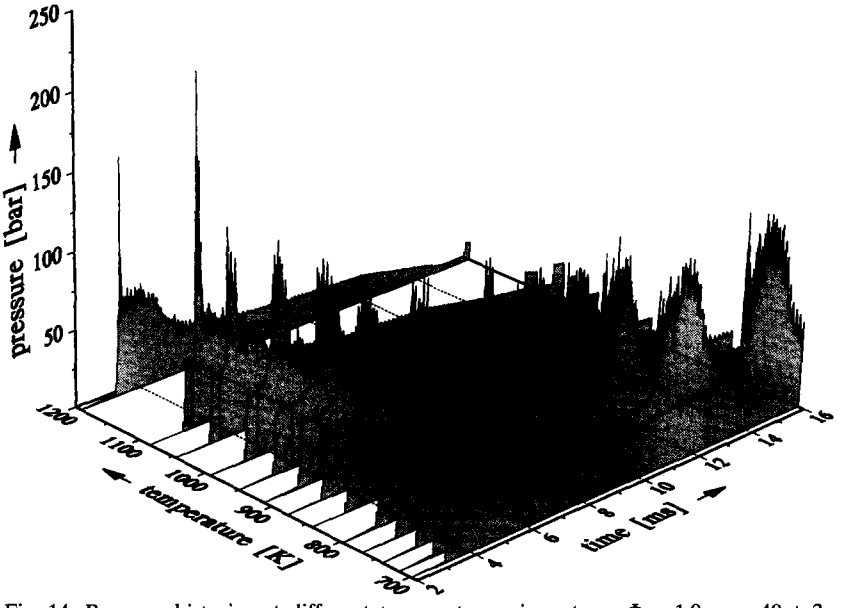

Fig. 14. Pressure histories at different temperatures, *iso*-octane, $\Phi = 1.0$, $p = 40 \pm 2$ bar. Vertical lines inside shaded area under pressure profiles mark instant of mild ignition. Signals were obtained at 15 mm in front of end wall.

$< \approx 800$ K at higher pressures (34 bar and 40 bar), the transition from a high to a low temperature kinetic system is connected with a two-step cool flame ignition process. The corresponding delay times, τ_1, of the cool flame process are also included in Fig. 10. For stoichiometric mixtures, this is not very pronounced and can be identified mainly by the emission signals. For rich mixtures, a step-like pressure increase similar to the initiation of the cool flame processes of *n*-heptane [8], can be observed.

In Figs. 15 and 16, *iso*-octane results for $p = 40 \pm 2$ bar are compared for different values of the equivalence ratio, Φ. For rich ($\Phi = 2.0$) and lean ($\Phi = 0.5$) mixtures, there was no evident pressure increase during the initial deflagration phase. Also, the band emission signals of the lean and rich mixture are very weak compared to the stoichiometric mixture. The delay times, τ_{defl} and τ_{DDT}, appear to differ for lean and rich mixtures less than is the case for stoichiometric mixtures. Hence, the ignition delay times, τ_{DDT}, for $\Phi = 0.5$ and $\Phi = 2.0$ are a suitable approximation for the chemical ignition delay in the whole temperature range of investigation. It can be supposed that the lower flame velocity for lean and rich mixtures [28] is the cause of this behaviour.

The values of τ_{DDT} in Fig. 15 show a pronounced negative temperature coefficient (NTC) behaviour for rich mixtures ($\Phi = 2.0$). There is a local maximum of the ignition delay time at $T \approx 850$ K and a minimum at $T \approx 750$ K. This transition to a low temperature kinetic system is very similar to recent results for *n*-heptane [8], and is also connected to the initiation of a cool flame reaction process (τ_1 in Fig. 15). The ignition delay times increase with decreasing equivalence ratio. In the temperature range between 800 and 1050 K, the delays, τ_{DDT}, of the stoichiometric mixtures are shortened by the influence of the deflagration process, as previously described. Because of this, the times, τ_{DDT}, for stoichiometric mixtures are shorter than those for $\Phi = 2.0$, which is not conclusive from the kinetic point of view. If the values of τ_{DDT} for $\Phi = 1.0$ are re-evaluated using Eq. 1, the ignition delays are longer than those of rich mixtures and also lead to a NTC behaviour. This, however, is less pronounced than for rich mixtures.

At lower pressures (13 bar), the results for the several non-stoichiometric equivalence ra-

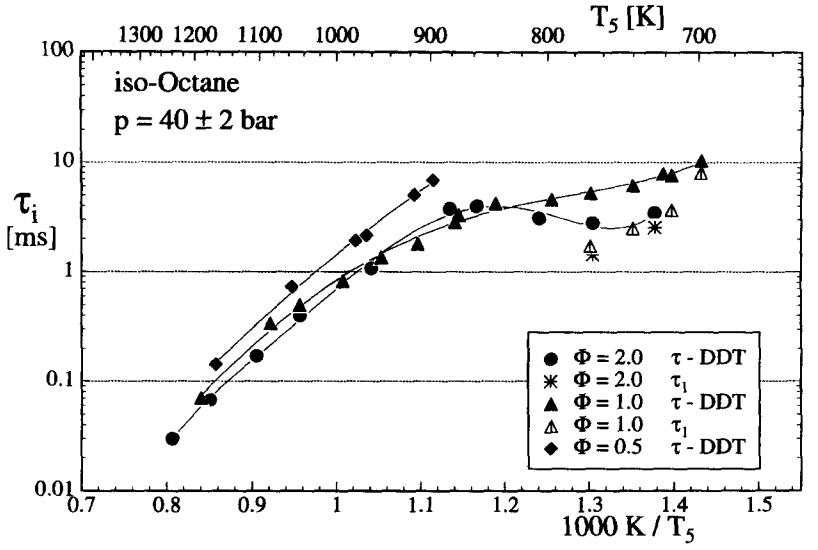

Fig. 15. Ignition delay time, τ_{DDT}, and cool flame delay, τ_l, at different equivalence ratios, *iso*-octane, $p = 40 \pm 2$ bar.

tios do not differ much from the stoichiometric results, as only the high temperature region could be covered, due to the long ignition delay times. At this pressure, investigations with rapid compression machines also have been described [29–31]. These results, contiguous to the data in the present study, extend to longer ignition delay times and lower temperatures.

Mixtures of *iso*-Octane and *n*-Heptane

In addition to the pure primary reference fuels (PRF), the self-ignition of their mixtures is of basic importance. Stoichiometric mixtures employed were: 60% *iso*-octane/40% *n*-heptane; 80% *iso*-octane/20% *n*-heptane, and 90% *iso*-octane/10% *n*-heptane. The results for a pressure of 40 ± 2 bar are presented in Figs.

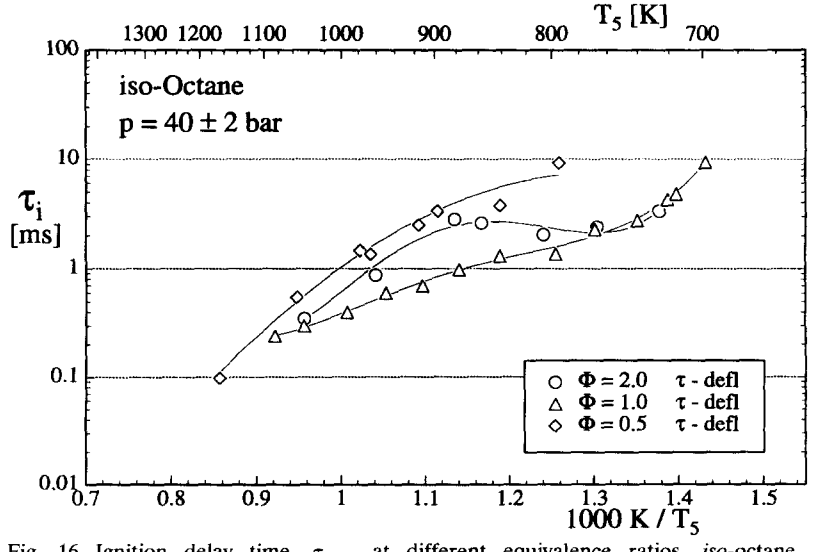

Fig. 16. Ignition delay time, τ_{defl}, at different equivalence ratios, *iso*-octane, $p = 40 \pm 2$ bar.

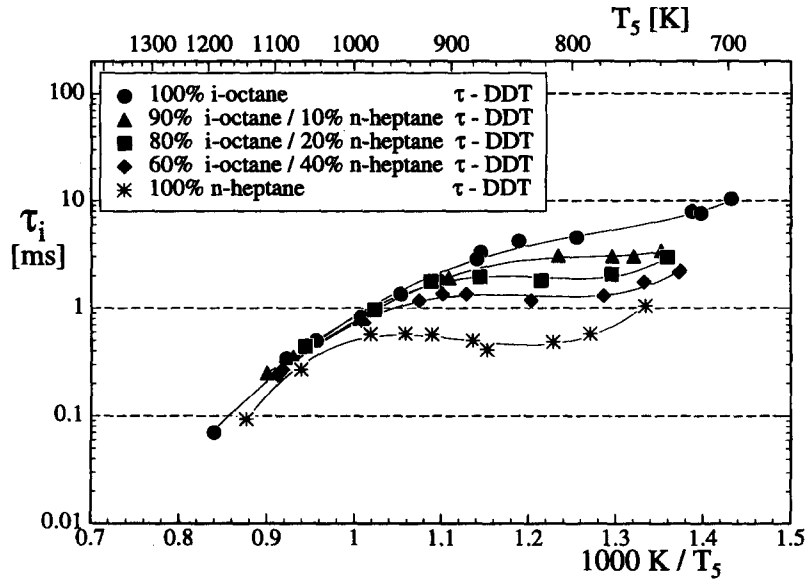

Fig. 17. Ignition delay time, τ_{DDT}, of *iso*-octane, *n*-heptane and different mixtures of both fuels, $\Phi = 1.0$, $p = 40 \pm 2$ bar.

17–19 and compared with results for the pure fuels. The *n*-heptane data were partially taken from [8], but were extended to lower temperatures by further measurements. Here, no values of τ_{defl}, were determined, as the mild self-ignition process was always followed directly by a strong ignition. As expected, the data for these mixtures are located within the range limited by the pure fuels. For temperatures above 1000 K, there is no significant difference between the ignition-delay times of the mixtures and pure *iso*-octane.

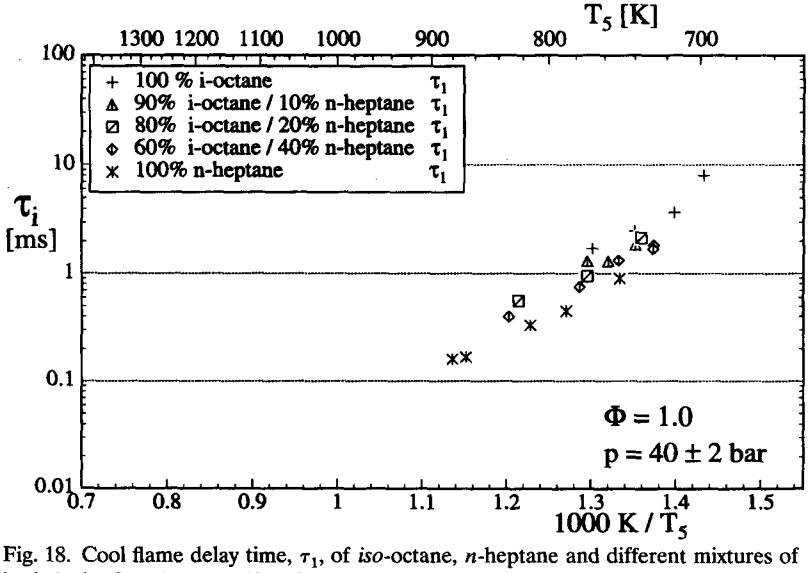

Fig. 18. Cool flame delay time, τ_1, of *iso*-octane, *n*-heptane and different mixtures of both fuels, $\Phi = 1.0$, $p = 40 \pm 2$ bar.

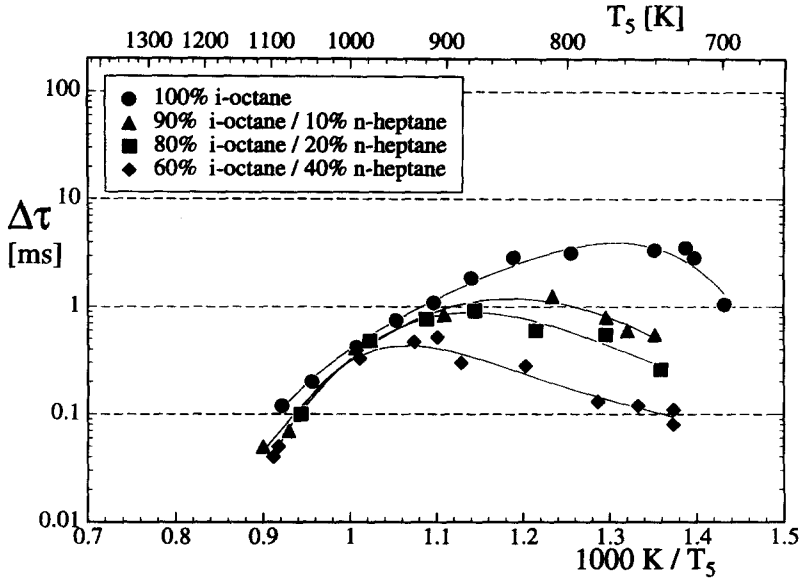

Fig. 19. Transition time, $\Delta\tau = \tau_{DDT} - \tau_{defl}$, of *iso*-octane and different mixtures of *iso*-octane and *n*-heptane, $\Phi = 1.0$, $p = 40 \pm 2$ bar.

As for *iso*-octane, a mild ignition is observed in the temperature range 800–1000 K. The deflagrative phase becomes shorter with an increasing *n*-heptane fraction. Also a pressure increase, due to deflagration, led to a shortening of the ignition delay time, τ_{DDT}, in this temperature range, as discussed previously for *iso*-octane.

For temperatures below about 900 K, a more or less S-shaped dependence (NTC) of τ_{DDT} can be observed in Fig. 17. This is very pronounced for *n*-heptane, but is less so than for *iso*-octane in this temperature range. Hence, lowering the *n*-heptane fraction in the mixtures reduced the NTC-behaviour, but it still is connected with a two-step ignition process. This cool flame process was observed also for mixtures containing only 10% *n*-heptane. The corresponding values of τ_1 can be found in Fig. 18. Hence, the self-ignition process of the mixtures at lower temperatures ($T < 900$ K) is mainly influenced by the low temperature kinetics of *n*-heptane.

The delay times of the mild ignition (τ_{defl}) vary less than the times, τ_{DDT}, for the different mixtures. Figure 19 shows the difference in ignition delay times, $\Delta\tau = \tau_{DDT} - \tau_{defl}$, from the occurrence of the first kernels to the secondary explosion. These transition times are identical for pure *iso*-octane and the mixtures at temperatures above 1000 K. At lower temperatures, the influence of the *n*-heptane fraction in the mixtures led to a much faster transition to a detonative main ignition.

Methanol and Methyl *tert*-Butyl Ether

For various reasons, methanol may become an important alternative fuel. Due to its high octane number (RON: 114, MON: 94), it can be used as an SI engine fuel or as a fuel component. Stoichiometric methanol/air mixtures were investigated at pressures of 13 ± 1.5 bar and 40 ± 2 bar. The results are shown in Fig. 20, in which τ_{DDT} and τ_{defl} are plotted.

Methyl *tert*-Butyl Ether (MTBE) is increasingly used as a knock resistant fuel component (RON: 116, MON: 100), replacing benzene and lead compounds. The results obtained for MTBE are presented in Fig. 21. They are very similar to those for methanol. Comparison of Figs. 20 and 21 shows the ignition delay times of methanol to be slightly shorter over the whole temperature range. For both fuels, the mild ignition led to an extended deflagrative phase for temperatures smaller than 1000 K.

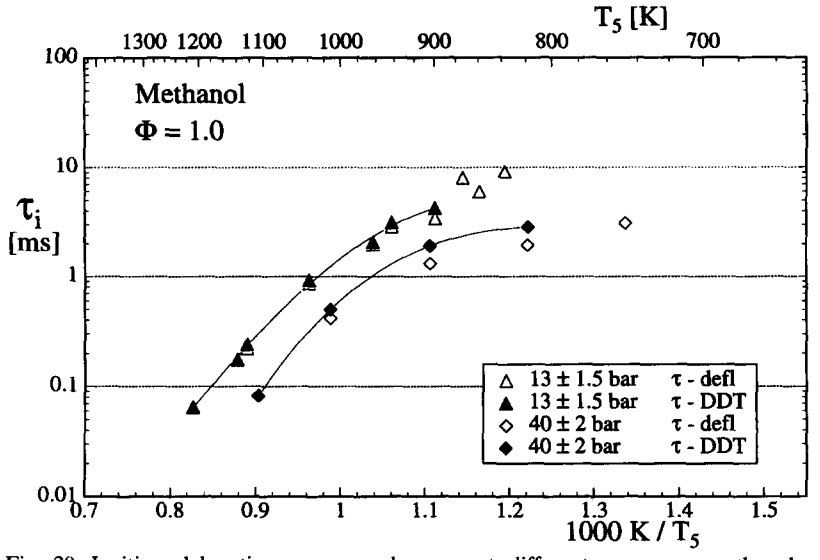

Fig. 20. Ignition delay times, τ_{defl} and τ_{DDT}, at different pressures, methanol, $\Phi = 1.0$.

Below a temperature of ~ 900 K (methanol, $p = 40$ bar: 800 K), no secondary explosion could be observed.

The ignition delay times of both fuels must be assessed in relation to the experimental pressure histories. As an example, the measured results for MTBE at $p = 40 \pm$ bar are presented in Fig. 22. The results for methanol and for the experiments at lower pressures are qualitatively very similar. Again, a pronounced deflagrative phase with a pressure increase of up to twice the value of the initial pressure after compression was observed. If for both fuels—under constant pressure conditions—a straight dependence of the chemical ignition delay time in the form of an Arrhenius function, $\tau_i = A \exp(k/T_5)$, is assumed, A and k can be determined by using Eq. 1 and the

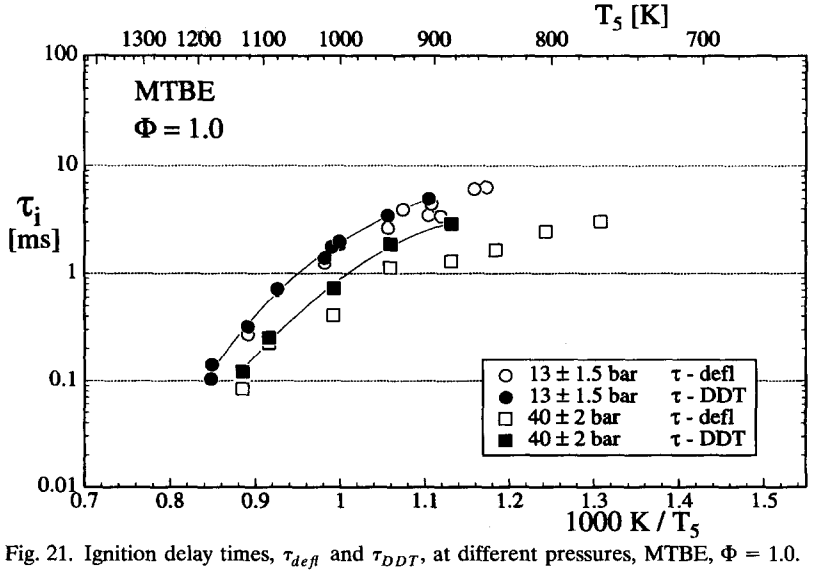

Fig. 21. Ignition delay times, τ_{defl} and τ_{DDT}, at different pressures, MTBE, $\Phi = 1.0$.

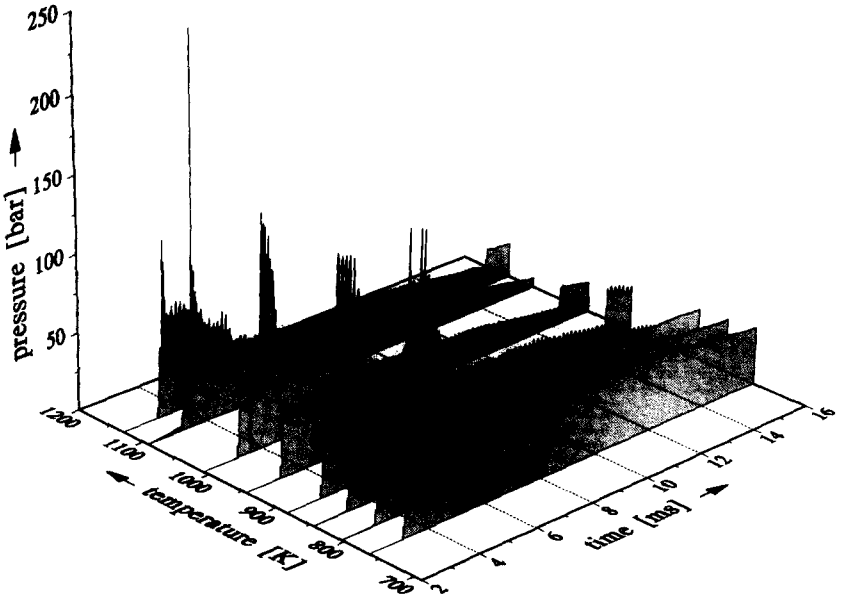

Fig. 22. Pressure histories at different temperatures, MTBE, $\Phi = 1.0$, $p = 40 \pm 2$ bar. Vertical lines inside shaded area under pressure profiles mark instant of mild ignition. Signals were obtained at 15 mm in front of end wall.

measured pressure histories, as described above. The results of this calculation ($\gamma = 1.27$) are presented in Fig. 23 for both fuels and $p = 40 \pm 2$ bar. The parameters A and k were adjusted such that for all experiments the integral in Eq. 1 was approximately equal to unity for τ_{DDT}. The dependence of the ignition delay times on the pressure was not taken into account in this first approach. Nevertheless, this estimate shows that the measured pressure increase arising from deflagration was able to shorten τ_{DDT} by up to one order of magnitude (methanol, $T = 800$ K, $p = 40$ bar). For all experiments without the occurrence of a secondary explosion, the value of the integral is evidently smaller than 1 at the end of the test

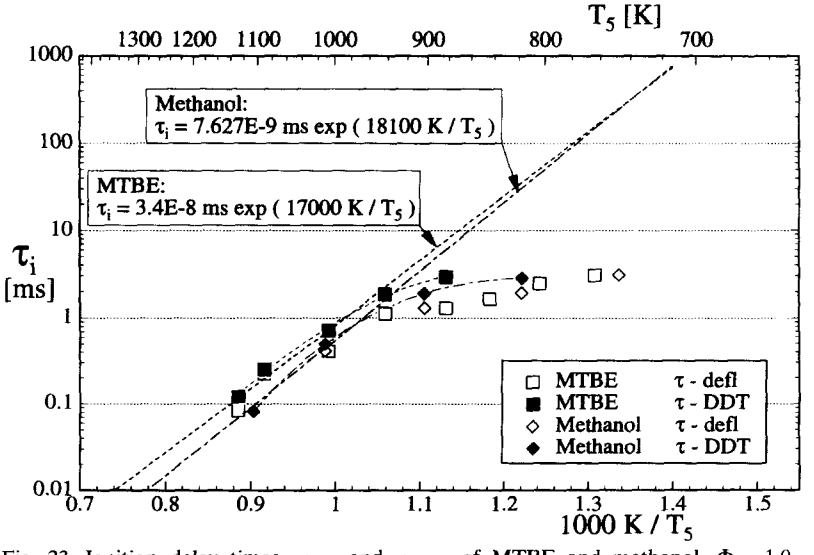

Fig. 23. Ignition delay times, τ_{defl} and τ_{DDT}, of MTBE and methanol, $\Phi = 1.0$, $p = 40 \pm 2$ bar. Dashed lines represent assumed dependence, $\tau_i = f(T)$.

time after 12 ms. Hence, the supposed linear dependence of τ_i in the Arrhenius plot seems to be conclusive within the investigated temperature range, which is not obvious solely from the measured results.

The long ignition delay times leading to an inhomogeneous mild self-ignition and the absence of the transition into low temperature chemistry with NTC, seem to be responsible for the good anti-knock properties of the two fuels.

CONCLUSIONS

The self-ignition process of several SI engine model fuels, mixed with air, has been investigated experimentally under engine-relevant conditions, by the shock tube technique. The fuels were *iso*-octane, methanol and methyl *tert*-butyl ether. To gain further information about the influence of the octane number on the self-ignition process, three different mixtures of the primary reference fuels, *iso*-octane and *n*-heptane, were investigated.

Typical models of the self-ignition process have been photographed with a shock tube equipped with large windows along the test section and high-speed shadowgraphs obtained (see, also, [18]). These experiments show that for temperatures relevant to piston engine combustion, the self-ignition process always starts in an inhomogeneous, deflagrative manner. This mild ignition, arising from the local self-ignition of very small volumes of the test gas (hot spots), leads to deflagrative combustion and may cause a consecutive moderate pressure increase. The beginning of the deflagrative phase is accompanied by emission from the CH-band at 431 nm, and this was used to determine a first ignition delay time, τ_{defl}.

The deflagration process, in most cases, was followed by a secondary, nearly homogeneous self-ignition of a larger volume of the still unburned test gas. This secondary explosion is connected with shock waves, which can be seen clearly in the pressure records. A second ignition delay time, τ_{DDT}, has been defined using this instant of the secondary explosion. This time can be used as a suitable approximation for the chemical ignition delay time, if the change of the thermodynamic conditions of the unburned test gas, due to the pressure increase arising from deflagration, is taken into account.

At low temperatures, a homogeneous cool flame process can be observed for some fuels. This is reflected both in the pressure and emission signals, which were used to obtain a cool flame delay time, τ_1. A typical record of the CH-band emission and pressure history showing all these features is given in Fig. 9.

In this manner, self-ignition has been investigated, in particular for high pressures, with a specially designed shock tube. For *iso*-octane at $p = 40$ bar, a NTC (negative temperature coefficient) behaviour connected with a two-step (cool flame) self-ignition at low temperatures could be observed. This process was very pronounced for rich, and less pronounced for stoichiometric mixtures. The results of the τ_{DDT} delays of the stoichiometric mixtures were shortened by the primary deflagration process in the temperature range between 1000 and 800 K.

Various mixtures of *iso*-octane and *n*-heptane were investigated in order to clarify the influence of the octane number both on the ignition delay time and on the mode of self-ignition. All mixtures showed a more or less pronounced NTC behaviour in dependence on the *n*-heptane fraction. At low temperatures, two-step cool flame pre-ignition occurred, even for the RON 90 mixture. With an increasing *n*-heptane fraction in the mixtures, the mild self-ignition process changed faster into a detonative mode, which partially is the reason of the distinct decrease in ignition delay times, τ_{DDT}. At higher temperatures, the self-ignition of the mixtures proceeded—similar to *iso*-octane—with a more extended deflagrative phase prior to a secondary explosion.

Finally, methanol and methyl *tert*-butyl ether, both of which have a high octane number, have been investigated. The self-ignition of both fuels is characterized by a very pronounced initial deflagration. For temperatures below 900 K (methanol: 800 K), no secondary explosion occurred. Taking into account the pressure increase due to deflagration, the measured delays, τ_{DDT}, of the secondary explosion were shortened by up to one order of magnitude. This is demonstrated by the approximately lin-

ear dependence of the chemical ignition delay time in the Arrhenius plot for temperatures higher than 800 K.

This work was supported by the German Science Foundation DFG as a project of the Sonderforschungsbereich 224 "Motorische Verbrennung".

REFERENCES

[1] Miller, C. D. *SAE Quarterly Transactions* 1 (1947).
[2] Male, T. *Third Symposium on Combustion and Flame and Explosion Phenomena* 1949.
[3] König, G., and Sheppard, C. G. W., SAE Paper No. 902135, 1990.
[4] König, G., Maly, R. R., Bradley, D., Lau, A. K. C., and Sheppard, C. G. W., SAE Paper No. 902136, 1990.
[5] Spicher, U., Kröger, H., and Ganser, J., SAE Paper No. 912312, 1991.
[6] Stiebels, B., Sakak, S., and Schreiber, M., SAE Paper No. 960287, 1996.
[7] Ciezki, H. K., and Adomeit, G. *Seventeenth International Symposium on Shock Tubes and Waves, AIP Conference Proceedings*, Vol. 208, (Y. W. Kim, Ed.), 1989, p. 707.
[8] Ciezki, H. K., and Adomeit, G. *Comb. Flame* 93:412–433 (1993).
[9] Ciezki, H. K., and Adomeit, G. *Deutscher Flammentag*. VDI Berichte 922, VDI Verlag Düsseldorf, 1991, pp. 495–503.
[10] Chevalier, C., Louessard, P., Müller, U. C., and Warnatz, J. *COMMODIA 90: Int. Symp. on Diagnostics and Modeling of Combustion in Internal Engines*, JSME, 1990.
[11] Müller, U. C., Peters, N., and Liñán, A. *Twenty-Fourth Symposium (International) on Combustion*. The Combustion Institute, Pittsburgh, 1992.
[12] Fieweger, K., Ph.D. thesis, RWTH Aachen, 1996.
[13] Fieweger, K., Blumenthal, R., and Adomeit, G. *Twenty-Fifth Symposium (International) on Combustion*. The Combustion Institute, Pittsburgh, 1994.
[14] Kee, R. J., Rupley, F. M., and Miller, J. A. *CHEMKIN II*: a FORTRAN Chemical Kinetics Package for the Analysis of Gas Phase Chemical Kinetics, Technical Report SAND89–8009B, UC–706, Sandia Nat. Lab, 1993.
[15] Lee, B. I., and Kesler, M. G. *AIChE Journal.* 21 (1975).
[16] Vermeer, D. J., Meyer, J. W., and Oppenheim, A. K. *Comb. Flame* 18:327–336 (1972).
[17] Oppenheim, A. K. *Phil. Trans. R. Soc. Lond.* A 315:471–508 (1985).
[18] Blumenthal, R., Fieweger, K., Komp, K. H., and Adomeit, G. *Fifteenth International Symposium on the Dynamics of Explosions and Reactive Systems*, Boulder, 1995. Accepted for publication in: *Combust. Sci. Technol.*
[19] Weber, Y. S., Oran, W. S., Boris, J. P., and Anderson, J. D., Jr. *Twentieth International Symposium on Shock Waves* 1995.
[20] Blumenthal, R., Ph.D. thesis, RWTH Aachen, 1996.
[21] Elsworth, J. E., Haskell, W. W., and Read, I. A. *Comb. Flame* 13:437 (1969).
[22] Haskell, W. W., SAE Paper No. 700059, 1970.
[23] Griffiths, J. F., Halford-Maw, P., and Rose, D. J. *Comb. Flame* 95:291–306 (1993).
[24] Strehlow, R. A. *Combustion Fundamentals*. McGraw Hill, New York, 1984.
[25] Heywood, J. B. *Internal Combustion Fundamentals*. McGraw-Hill, New York, 1988.
[26] Minetti, R., Carlier, M., Ribaucour, M., Therssen, E., and Sochet, L. R. *Combust. Flame* 102:298–309 (1995).
[27] Metghalchi, M., and Keck, J. C. *Comb. Flame* 48:191–210 (1982).
[28] Voinov, A. N., Skorodelov, D. I., and Sokolov, F. P. *Kinetika i Kataliz.* 5:388–398 (1964).
[29] Halstead, M. P., Kirsch, L. J., and Quinn, C. P. *Comb. Flame* 30:45–60 (1977).
[30] Minetti, R., Ribaucour, M., Carlier, M., and Sochet, L. R. *Fifteenth International Colloquium on the Dynamics of Explosions and Reactive Systems*. 1995.